Contents lists available at ScienceDirect

Estuarine, Coastal and Shelf Science

Phytoplankton community adaptation to changing light levels in the southern Beaufort Sea, Canadian Arctic

Atsushi Matsuoka [a,*], Pierre Larouche [b,1], Michel Poulin [c,2], Warwick Vincent [d,3], Hiroshi Hattori [e,4]

[a] Laboratoire d'Océanographie de Villefranche, Centre National de la Recherche Scientifique, Université Pierre et Marie Curie (Paris 6), B.P.08, Port de la Darse, Villefranche-sur-Mer Cedex, 06230 France
[b] Maurice Lamontagne Institute, Fisheries and Oceans Canada, 850 route de la Mer, P.O. Box 1000, Mont-Joli, Québec, G5H 3Z4 Canada
[c] Research Division, Canadian Museum of Nature, P.O. Box 3443, Ottawa K1P 6P4, Canada
[d] Départment de Biologie & Centre d'Études Nordiques, Université Laval, Québec G1K 7P4, Canada
[e] Department of Marine Biology and Sciences Tokai University, Minamisawa, Minami-ku, Sapporo 005-8601, Japan

ARTICLE INFO

ABSTRACT

The chlorophyll a specific absorption coefficient of phytoplankton, $a_\varphi^*(\lambda)$ is an important parameter to determine for primary production models and for the estimation of phytoplankton physiological condition. Knowledge of this parameter at high latitudes where nutrient rich cold water submitted to low incident light is a common environment is almost nonexistent. To address this issue, we investigated the light absorption properties of phytoplankton as a function of irradiance, temperature, and nutrients using a large data set in the southern Beaufort Sea during the open water to ice cover transition period. The $a_\varphi^*(\lambda)$ tended to increase from autumn when open water still existed to early winter when sea ice cover was formed, resulting from a biological selection of smaller-size phytoplankton more efficient to absorb light. There was no significant correlation between $a_\varphi^*(\lambda)$ and irradiance or temperature for both seasons. However, $a_\varphi^*(\lambda)$ showed a significant positive correlation with $NO_3 + NO_2$. Implications of the results for phytoplankton community adaptation to changing light levels are discussed.

© 2009 Elsevier Ltd. All rights reserved.

1. Introduction

The southern Beaufort Sea is characterized by the presence of the Mackenzie shelf having a depth of less than 80 m (Fig. 1). Even though this shelf accounts for only a few percent of the total Arctic Ocean surface area it receives a large amount of freshwater from the Mackenzie River estimated at $330 \, km^3 \, yr^{-1}$ (Stein and Macdonald, 2004). This flux contributes to the heat and nutrient supply to the Arctic Ocean (Aagaard and Carmack, 1989), and sustains biological activity from lower (phytoplankton) to higher trophic levels (fish, seabirds, and marine mammals) (Carmack and Macdonald, 2002).

In terms of bottom-up control, knowledge of phytoplankton biomass variability that allows estimating primary production (PP)

is thus important to understand the carbon cycle in the Arctic Ocean. In addition to irradiance, the chlorophyll a (chl a) specific absorption coefficient of phytoplankton ($a_\varphi^*(\lambda)$, $m^2 \, mg \, chl \, a^{-1}$) that is a light absorption capacity by phytoplankton for photosynthesis is a key factor to estimate PP (Platt and Sathyendranath, 1988; Sathyendranath et al., 1991; Longhurst et al., 1995; Arrigo et al., 1998) and to examine the physiological condition of phytoplankton (e.g., Morel and Bricaud, 1981; Mitchell and Holm-Hansen, 1987; Morel, 1991; Stramski and Reynolds, 1993; Bricaud et al., 1995; Cota et al., 2003; Matsuoka et al., 2006). Using a large lower latitudes data set ($N = 815$), Bricaud et al. (1995) suggested that smaller $a_\varphi^*(\lambda)$ is related to eutrophic conditions of water, where large-size phytoplankton such as diatoms dominate, leading to packaged phytoplankton light absorption (so called the packaging effect). While the intensity of light is also expected to be important for $a_\varphi^*(\lambda)$, the relationship between the two had not been examined by Bricaud et al. (1995).

Knowledge of $a_\varphi^*(\lambda)$ with varying light intensity has mostly been accumulated during laboratory experiments. These studies particularly focused on the diel variations of $a_\varphi^*(\lambda)$ using relatively high water temperature ($>20 \, °C$), sufficient nutrients, and irradiance up to $970 \, \mu mol \, quanta \, m^{-2} \, s^{-1}$ on batch culture of a single species (e.g., Stramski and Reynolds, 1993; Claustre et al., 2002; Ohi et al.,

* Corresponding author.
 E-mail addresses: atsushi.matsuoka@obs-vlfr.fr (A. Matsuoka), pierre.larouche@dfo-mpo.gc.ca (P. Larouche), mpoulin@mus-nature.ca (M. Poulin), warwick.vincent@bio.ulaval.ca (W. Vincent), hattori@dm.htokai.ac.jp (H. Hattori).
 [1] Tel.: +1 418 775 0569; fax: +1 418 775 0546.
 [2] Tel.: +1 613 566 4788; fax: +1 613 364 4027.
 [3] Tel.: +1 418 656 5644; fax: +1 418 656 2043.
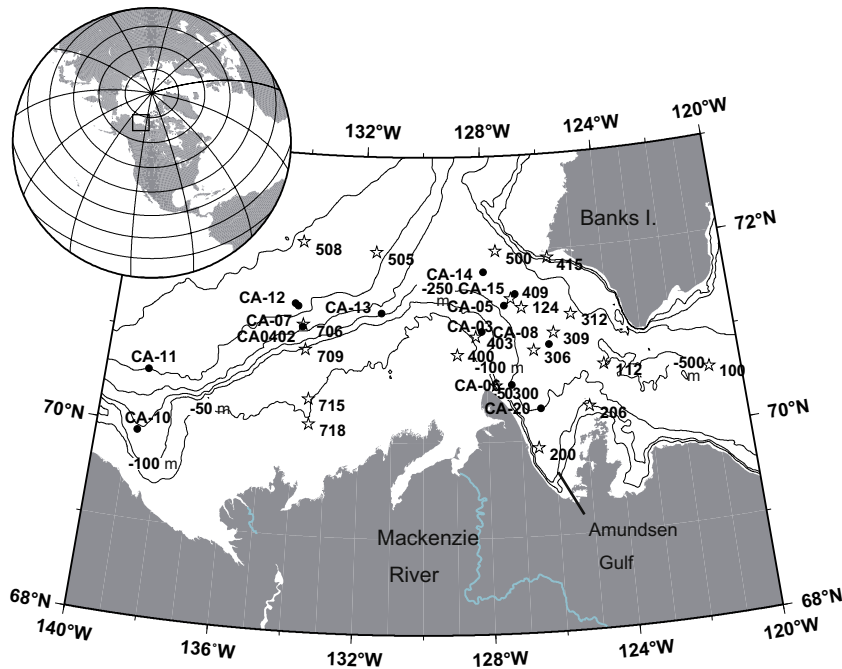 [4] Tel.: +81 11 571 5111; fax: +81 11 571 7879.

Fig. 1. Locations and station numbers for the CASES2003 cruise in the southern Beaufort Sea. Dots represent stations in leg 1 and stars in leg 2.

2006). These experiments showed that $a_\varphi^*(\lambda)$ can be maximal around sunset and minimal around sunrise due to change of pigment composition (Claustre et al., 2002). In open oceanic waters, Fujiki and Taguchi (2002) reported that variability in $a_\varphi^*(\lambda)$ as a function of irradiance is dependent on the physiological characteristics of marine phytoplankton. The behavior of $a_\varphi^*(\lambda)$ at high latitudes where nutrient rich cold water under low incident light is a common environment (Harrison and Cota, 1991) and where a variety of phytoplankton species exist (e.g., Cota et al., 2003; Lovejoy et al., 2007) could thus be different from that at lower latitudes.

The objective of this study is therefore to clarify the variability of phytoplankton light absorption properties with light, temperature, and nutrients in a polar environment. To completely describe the light absorption properties by all optical components, absorption coefficients of non-algal particles (NAP) and colored dissolved organic matter (CDOM) are also examined. This study focuses on the optical properties variability during the early winter transition period when sea ice cover is formed and should allow us to understand the behavior of absorption properties of phytoplankton for polar waters that are covered by sea ice for a great part of the year.

2. Materials and methods

Field observations were made in the southern Beaufort Sea and the Amundsen Gulf (Fig. 1) as part of the Canadian Arctic Shelf Exchange Study (CASES) 2003 expedition. Samples were collected during the first two legs of the expedition from 13 September to 14 October 2003 (leg 1) and from 15 October to 25 November 2003 (leg 2) onboard the Canadian icebreaker *CCGS Amundsen*. While open water still existed during leg 1, the study region was covered by newly formed sea ice during leg 2.

Temperature and salinity profiles were obtained using a SeaBird 911 Conductivity–Temperature–Depth (CTD) probe. Nutrient concentrations (nitrate plus nitrite, phosphate, and silicate) were determined on fresh samples (within 1 h of sampling) using

standard colorimetric methodologies (Grasshoff, 1999) adapted for use on an Auto-Analyzer 3 (Bran + Luebbe). During our cruise, a RAMSES ASC scalar hyperspectral irradiance sensor (TriOS) was mounted on the flight bridge to measure downwelling irradiance ($E_d(\lambda)$, $\mu W\,m^{-2}\,nm^{-1}$) with 1 nm intervals during the day. The *in situ* photosynthetically available radiation (PAR) was calculated by summing $E_d(\lambda)$ from 400 to 700 nm at solar noon, and used as a proxy of the incident light level (expressed in μmol quanta $m^{-2}\,s^{-1}$).

2.1. Absorption analysis

A total of 50 and 102 discrete water samples were collected at 13 and 20 stations for legs 1 and 2, respectively for chl *a* measurements and absorption analysis. The samples were taken over the euphotic zone (z_e, m) defined as the depth of the 1% surface light level measured using a PAR sensor attached to the CTD probe. One optical depth (z_{90}, m) that corresponds to the layer from which 90% of the upwelling radiance originates (Gordon and McCluney, 1975) was calculated as $1/z_e$. Onboard the ship, water samples were processed immediately after collection within 2 h for absorption analysis and 24 h for chl *a* measurements.

Chl *a* was determined fluorometrically with 90% acetone (Holm-Hansen et al., 1965) using a 10-AU field fluorometer (Turner Designs). For absorption analysis, water samples were filtered under low vacuum on Whatman GF/F glass fiber filters immediately after data collection. Optical density (OD, dimensionless) (Kirk, 1994) of all particles (phytoplankton plus NAP) on these filters, $OD_p(\lambda)$, was then measured from 400 to 750 nm with 1 nm intervals using a MPS2400 spectrophotometer (Shimazu corp.). Phytoplankton pigments were extracted using methanol (Kishino et al., 1985), and the OD of NAP, $OD_{NAP}(\lambda)$, was measured in the same way as for $OD_p(\lambda)$. The OD of phytoplankton, $OD_\varphi(\lambda)$, was obtained subtracting $OD_{NAP}(\lambda)$ from $OD_P(\lambda)$. Using the coefficients for β correction proposed by Cleveland and Weidemann (1993), these OD values were converted to absorption coefficients of phytoplankton ($a_\varphi(\lambda)$, m^{-1}) and NAP ($a_{NAP}(\lambda)$, m^{-1}) with 750 nm as

baseline for both. The $a_\varphi^*(\lambda)$ was calculated dividing $a_\varphi(\lambda)$ by chl a concentration. Mean values and standard deviations of $a_\varphi(\lambda)$ and $a_\varphi^*(\lambda)$ spectra were computed using all data for each leg. For absorption measurement of CDOM, water samples were first filtered using a 0.22 µm Millipore membrane. The OD of CDOM, $OD_{CDOM}(\lambda)$, was measured from 400 to 700 nm with 1 nm intervals using a MPS2400 spectrophotometer (Shimazu corp.) with the 700 nm value used as baseline. The $a_{CDOM}(\lambda)$ (m^{-1}) was then calculated as follow:

$$a_{CDOM}(\lambda) = 2.303 \frac{OD_{CDOM}(\lambda)}{0.1} \tag{1}$$

where 2.303 is a factor for converting base e to base 10 logarithms, and 0.1 is optical pathlength. Total non-water absorption coefficient, $a_{t-w}(\lambda)$ (m^{-1}) was calculated as the sum of $a_\varphi(\lambda)$, $a_{NAP}(\lambda)$, and $a_{CDOM}(\lambda)$.

2.2. Discrimination of phytoplankton taxa and HPLC pigment analysis

Water samples for cell identification and enumeration were preserved in acidic Lugol solution (Parsons et al., 1984) and stored in the dark at 4 °C until analysis. Samples were enumerated and identified to the lowest possible taxonomic rank using an inverted microscope (WILD Heerbrugg) operating with phase contrast optics (Utermöhl, 1931; Lund et al., 1958). The main taxonomic references according to Tomas (1997) and Bérard-Therriault et al. (1999) were used for phytoplankton identification.

Detailed method for high performance liquid chromatography (HPLC) pigment analysis is described in Lovejoy et al. (2007). Briefly, 1–2 L water samples were filtered on a Whatman GF/F glass fiber filter immediately after collection. The filters were then stored frozen at −80 °C until analysis. Phytoplankton pigments were extracted in 3 ml of 95% methanol. 50–100 µL of the extracts were then measured using a ProStar HPLC (Varian Inc.) equipped with a Symmetry C8 column (3.5 µm pore-size, 4.6 mm × 150 mm; Waters Corp.). The HPLC peaks were detected from 350 to 750 nm at 1 nm intervals. Absorbance chromatograms were obtained at 440 (for chlorophylls) and 450 nm (for carotenoids). Chlorophylls were also detected by fluorescence (excitation: 440 nm; emission: 650 nm). Concentrations of chl a and chlorophyll b (chl b) were then obtained. These two pigments determined by HPLC measurements were used for the calculation of the ratios of chl b to chl a.

Table 1
Coefficients for power laws expressed as $a_\varphi(\lambda) = A_\varphi(\lambda)[chl\,a]^{E_\varphi(\lambda)}$ at 443 nm. Available coefficients from the literature are also shown for comparison.

		Layer	A_φ	E_φ	$r^2(\varphi)$	N
This study	leg 1	$<z_{90}$	0.0574	1.382	0.82	12
		$>z_{90}$	0.0238	0.710	0.88	19
		All	0.0303	0.841	0.81	31
	leg 2	$<z_{90}$	0.0631	1.001	0.87	39
		$>z_{90}$	0.0559	0.873	0.75	52
		All	0.0567	0.889	0.84	91
	Total					122
Literature	Matsuoka et al. (2007)		0.0288	0.820	0.80	183
	Cota et al. (2003)		0.0402	0.578	0.73	175
	Wang et al. (2005)		0.0151	0.957	0.89	157
	Bricaud et al. (1998)		0.0378	0.627	0.90	1166

2.3. Regression analysis

A power function was applied to examine the relationship between the absorption coefficient of phytoplankton, $a_\varphi(\lambda)$ and chl a (Bricaud et al., 1995, 1998), assuming that this function is appropriate for Arctic species:

$$a_\varphi(\lambda) = A_\varphi(\lambda)[chl\,a]^{E_\varphi(\lambda)} \tag{2}$$

where λ is the wavelength and $A_\varphi(\lambda)$ and $E_\varphi(\lambda)$ are empirically derived coefficients (see Table 1).

The $a_\varphi^*(\lambda)$ is tightly related to phytoplankton physiological parameters, the maximum photosynthetic rate (P_{max}) and the initial slope of the production versus irradiance (α) (e.g., Kirk, 1994; Falkowski and Raven, 1997). More recently, Huot et al. (2007) performed a stepwise regression analysis to examine which environmental parameter had more impact on P_{max} and α estimates. We thus adopted this analysis to examine which of light, temperature, and nutrient parameter was more related to $a_\varphi^*(\lambda)$ as follows:

$$\log_{10} a_\varphi^*(\lambda) = A + \sum_{i=1}^{N} B_i \cdot \log_{10} X_i \tag{3}$$

where A and B_i are empirically derived intercept and coefficient, respectively, and N is the number of ith parameters, X_i which is used in this analysis, except for temperature.

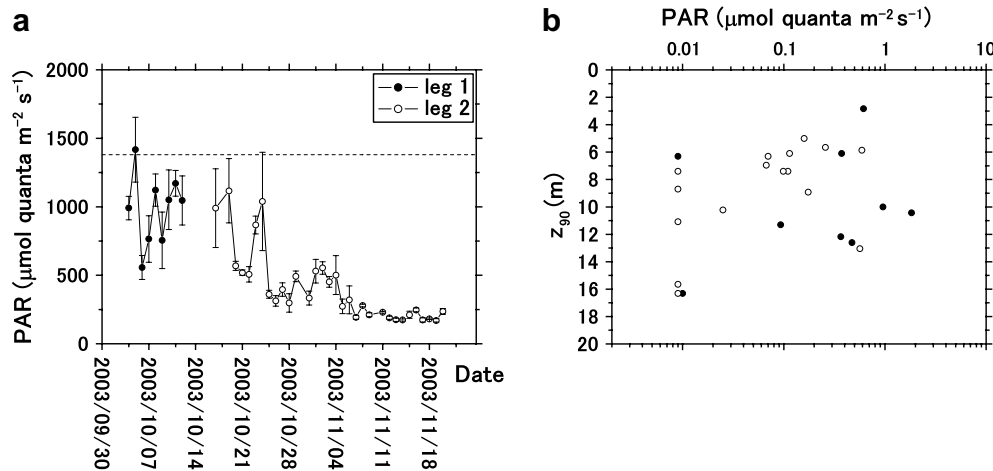In this study, T-test was performed to statistically quantify the fits obtained by the above regression analysis.

Fig. 2. Available light condition. (a) Variability in photosynthetically available radiation (PAR) at solar noon for leg 1 (closed circles) and leg 2 (open circle). The light intensity at moderate latitude, Tokyo bay on 16 October 1983 (Kishino, 1994) is shown as dashed line for comparison. (b) Location of z_{90} at which approximately 90% of upwelling radiance originates as a function of irradiance for leg 1 and leg 2.

3. Results and discussion

3.1. Light condition and the influence of the Mackenzie river freshwater plume

The light intensity primarily affects the phytoplankton growth and PP in general. We first examine the change in the incident light intensity during the cruise (Fig. 2). While a large variability in the light level due to the weather conditions was observed (i.e., mostly cloud-covered conditions with some sunny periods), the mean light intensity at the sea surface decreased with time to values around 200 μmol quanta m^{-2} s^{-1} (Fig. 2a). Compared to observations at moderate latitudes and at the same time period (1380 μmol quanta m^{-2} s^{-1} at the surface on 13 October 1983, Tokyo Bay; Kishino, 1994), the incident light was thus very low especially during leg 2. The light penetration depth was significantly higher during leg 1 ($P < 0.0001$) than during leg 2 for the same range of the incident light intensity (Fig. 2b).

Freshwater influences the optical properties through the presence of CDOM that absorbs light mostly in the blue part of the spectrum. The freshwater runoff of the Mackenzie river from autumn to early winter is relatively small but cannot be ignored (Carmack et al., 2004). Based on the presence of 26–28 practical salinity units (psu) as a definition of the edge of the Mackenzie plume (Carmack and Macdonald, 2002), we can see that during our sampling period, the Mackenzie river plume extended over a large area even reaching the Amundsen Gulf (Fig. 3) through either density driven or wind-induced local surface circulation patterns (Macdonald et al., 1987; Carmack and Macdonald, 2002; Macdonald and Yu, 2006). Influence of the runoff during our observation can also be seen using the relationship between $a_{CDOM}(412)$ and salinity (Fig. 4). The $a_{CDOM}(412)$ is inversely correlated with salinity up to about 28 (psu) when the linear relationship breaks due to chemical changes of CDOM (Nieke et al., 1997). This linear relationship is a well known phenomenon that has often been observed in a wide variety of estuaries and is consistent with previous results in this region (Bélanger et al., 2006). Most of the data points above 28 psu are located below z_{90} and are scattered largely indicating that the optical influence of the freshwater plume from the Mackenzie river is mostly constrained to the water layer above z_{90} (mean depth of 10 m; Fig. 2b) which is consistent with the results of Carmack et al. (2004).

3.2. Characteristics of light absorption coefficients of phytoplankton, NAP, and CDOM

We examined chl *a* values as a proxy of phytoplankton biomass during the sampling period (Fig. 5). The chl *a* values ranged from
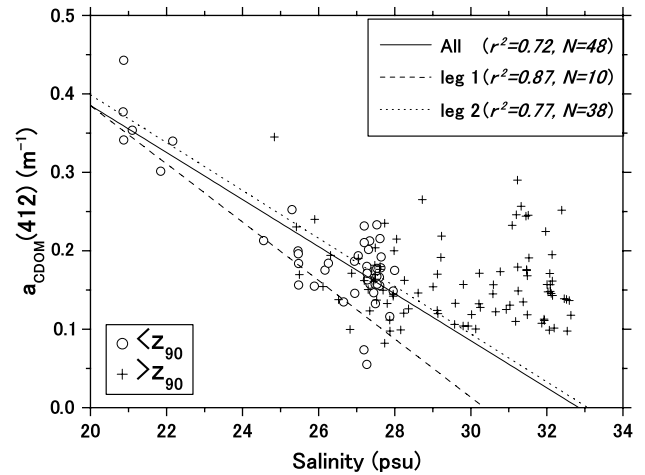

Fig. 4. Relationship between $a_{CDOM}(412)$ and salinity. Data are separated according to whether samples were taken above (open circle) or below (crossed mark) one optical depth (z_{90}). The fit for leg 1 and 2 (dashed and dotted lines, respectively) and all data (solid line) and correlation for data points above z_{90} are shown.

0.02 to 0.9 mg m^{-3} for both leg 1 and leg 2 indicating a low phytoplankton biomass. These values fall within the range reported at the same time of the year for the region west of the Mackenzie river mouth that includes the Chukchi and western Beaufort seas (Matsuoka et al., 2007).

We found a high correlation between $a_\varphi(\lambda)$ at 443 nm where phytoplankton absorption is maximal and chl *a* for both leg 1 and leg 2 ($r^2 = 0.81$ and 0.84, respectively; see Table 1 and Fig. 5). These high correlations between the two variables are consistent with previous reports from all latitudes (e.g., Bricaud et al., 1995, 1998; Cota et al., 2003; Wang et al., 2005; Matsuoka et al., 2007). During leg 1, the logarithmic slope of the relation is however much larger for the surface layer than for deeper layer (1.382 and 0.710, respectively; see Table 1) indicating an increased absorption capacity for the same chl *a* values. This vertical difference of $a_\varphi(443)$ was not observed for the region west of the Mackenzie river mouth (Matsuoka et al., 2007) indicating the optical specificity of our study area that results from the vertical stratification.

While the number of samples used for our analysis is limited for leg 1 ($N = 31$), the fit for all data points is very similar with the one obtained by Matsuoka et al. (2007) for the region west of the Mackenzie river mouth at the same time of the year (Fig. 5a). This result suggests that, when integrated over the euphotic zone, $a_\varphi(443)$ has the same characteristics for the entire western Arctic Ocean from autumn to early winter. Compared to other environments, $a_\varphi(443)$ is smaller than values measured in open oceanic
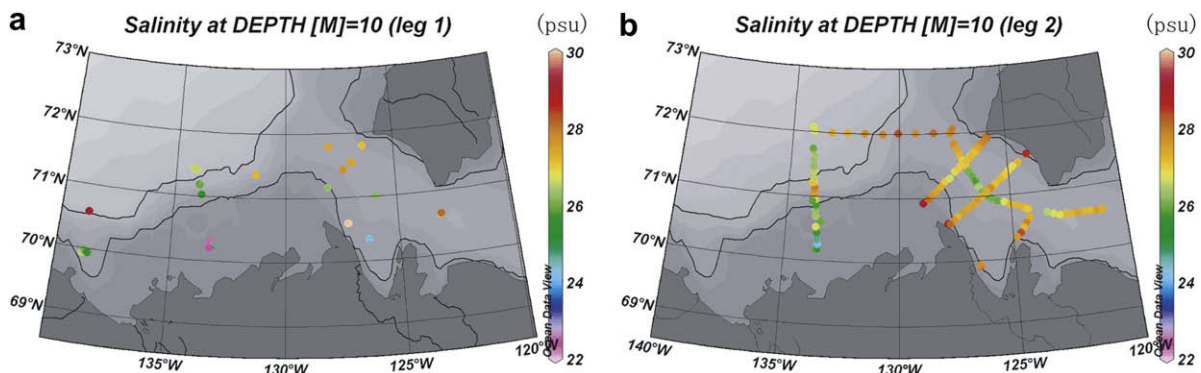

Fig. 3. Salinity (psu) at 10 m depth for leg 1 (left) and leg 2 (right).
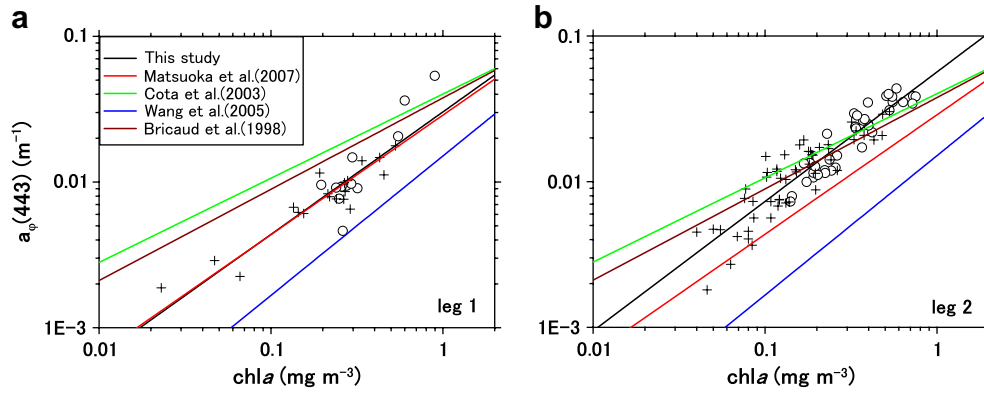
Fig. 5. Relationship between $a_\varphi(443)$ and chl a for (a) leg 1 and (b) leg 2. Regression lines of previous experiments are displayed for comparison. See Fig. 4 for symbols.

waters at lower latitudes (Bricaud et al., 1998) and in the Labrador Sea (Cota et al., 2003) at various seasons but larger than western Arctic values measured in summer (Wang et al., 2005) (Fig. 5a). It is interesting to note that $a_\varphi(443)$ increased from leg 1 to leg 2 and was higher than for the western Arctic at the same time period (Matsuoka et al., 2007), getting closer to values measured at lower and temperate latitudes (Fig. 5b). The strong vertical difference observed during leg 1 was much less for leg 2 (Table 1).

To examine the contribution of phytoplankton absorption to the other optical constituents, the relative proportion of the absorption coefficient by each optical component (phytoplankton, NAP, and CDOM) to the total non-water absorption, $a_{t-w}(\lambda)$ (see Table 2) are shown for five wavelengths that correspond to the spectral bands of the MODIS ocean color sensor (Fig. 6). In our study area, the maximum CDOM absorption at 443 nm was 0.29 m^{-1} which is comparable to measurements in other coastal environments (e.g., 0.27 m^{-1} for Chesapeake Bay; Kirk, 1994). The total non-water absorption coefficient is clearly dominated by CDOM for both legs and at all wavelengths (Fig. 6 and Table 2). This is very different from measurements done in the same area during summer (June and July) when $a_{CDOM}(443)$ only contributes approximately 50% to $a_{t-w}(443)$ (Bélanger et al., 2006). This observation is consistent with the larger impact of the Mackenzie river plume later in the season due to the time taken for water advection from the river mouth. The magnitude of NAP absorption was up to 0.09 m^{-1} and is second in importance for light absorption (Fig. 6; see Table 2 for details). This result is comparable to the one obtained in the region west of the Mackenzie river mouth where $a_\varphi(\lambda)$ is the second contributor to $a_{t-w}(\lambda)$ (Matsuoka et al., 2007). The magnitude of $a_{NAP}(\lambda)$ normally reflects the presence of suspended particles (Babin et al., 2003). Therefore, our results that show high contributions of CDOM and NAP absorption

to the total non-water absorption suggest that a strong influence of the Mackenzie river runoff still exists from autumn to early winter period over the whole area (see also Fig. 4). Although the contributions of $a_\varphi(\lambda)$ are small at that time of the year, it is worth noting that its proportion tends to increase from leg 1 to leg 2 (up to 25% at 443 nm: Fig. 6) resulting mostly from the reduced CDOM influence during the second leg.

3.3. Change of phytoplankton absorption spectra

Mean spectra of $a_\varphi(\lambda)$ and $a_\varphi^*(\lambda)$ for both legs are shown in Fig. 7. Despite a large variability, it is observed that $a_\varphi(\lambda)$ is generally higher during leg 2. The change of phytoplankton absorption is more clearly shown in the mean spectra of $a_\varphi^*(\lambda)$. These results indicate that $a_\varphi^*(\lambda)$, which provides an indication of *in vivo* absorption capacity of phytoplankton cells (Morel and Bricaud, 1981; Bricaud et al., 1995), was significantly higher during leg 2 ($P < 0.01$; Fig. 7c,d). Two possible causes are put forward to explain the observed change: a different phytoplankton species composition or an adaptation to a changing light condition by the same dominant species of phytoplankton.

Fig. 8 shows the mean phytoplankton species composition for both legs expressed as absolute abundance and relative percentages. During leg 1, no clear dominant species is present (Flagellates: $26 \pm 14\%$, Dinophyceae: $16 \pm 7\%$, Prasinophyceae: $14 \pm 8\%$, and Prymnesiophyceae: $13 \pm 7\%$). Our taxonomic data show that only two major phytoplankton species, Flagellates ($44 \pm 15\%$) and Prymnesiophyceae ($25 \pm 9\%$) increased their abundance significantly from leg 1 to leg 2 ($P < 0.01$ for Flagellates and $P < 0.001$ for Prymnesiophyceae) while all other species declined (Fig. 8a). The phytoplankton community thus changed with time with smaller

Table 2
Relative contributions of absorption coefficient of phytoplankton (φ), non-algal particles (NAP), and CDOM to the total non-water absorption, $a_{t-w}(\lambda)$ at 412, 443, 488, 531, and 551 nm that correspond to the spectral bands of the MODIS ocean color sensor. The average $\pm$ one standard deviation is shown. Available coefficients from the literature are also shown for comparison.

|	λ (nm)	leg 1 ($N = 50$)				leg 2 ($N = 102$)			
		$a_\varphi(\lambda)/a_{t-w}(\lambda)$	$a_{CDOM}(\lambda)/a_{t-w}(\lambda)$	$a_{NAP}(\lambda)/a_{t-w}(\lambda)$	$a_{t-w}(\lambda)$	$a_\varphi(\lambda)/a_{t-w}(\lambda)$	$a_{CDOM}(\lambda)/a_{t-w}(\lambda)$	$a_{NAP}(\lambda)/a_{t-w}(\lambda)$	$a_{t-w}(\lambda)$
This study	412	0.04 ± 0.02	0.87 ± 0.07	0.09 ± 0.05	0.22 ± 0.09	0.07 ± 0.03	0.79 ± 0.08	0.14 ± 0.07	0.22 ± 0.08
	443	0.07 ± 0.04	0.84 ± 0.08	0.09 ± 0.06	0.16 ± 0.07	0.11 ± 0.05	0.74 ± 0.09	0.15 ± 0.08	0.14 ± 0.05
	488	0.08 ± 0.05	0.82 ± 0.10	0.09 ± 0.07	0.09 ± 0.04	0.14 ± 0.06	0.70 ± 0.10	0.16 ± 0.09	0.08 ± 0.03
	531	0.07 ± 0.04	0.83 ± 0.11	0.11 ± 0.08	0.05 ± 0.02	0.12 ± 0.05	0.70 ± 0.11	0.19 ± 0.10	0.04 ± 0.01
	551	0.05 ± 0.04	0.83 ± 0.12	0.11 ± 0.09	0.04 ± 0.02	0.10 ± 0.04	0.70 ± 0.12	0.20 ± 0.11	0.03 ± 0.01
Literature									
Matsuoka et al. (2007)	443	0.16 ± 0.11	0.76 ± 0.13	0.08 ± 0.05					
Babin et al. (2003)		0.36 ± 0.14	0.41 ± 0.14	0.22 ± 0.13					
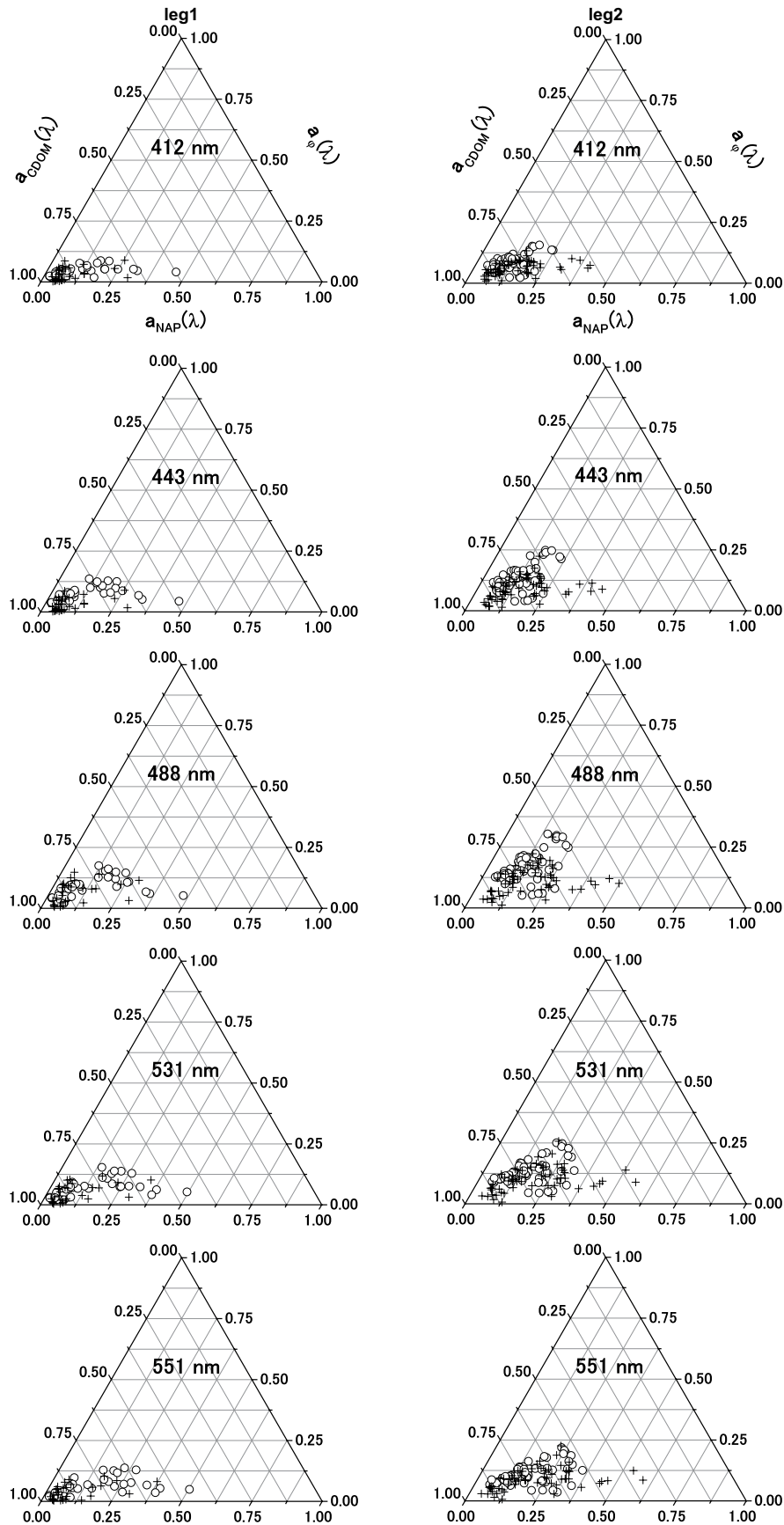
Fig. 6. The proportions of absorption coefficient of phytoplankton, NAP, and CDOM to the total non-water absorption at 412, 443, 488, 531, and 551 nm. See Fig. 4 for symbols.
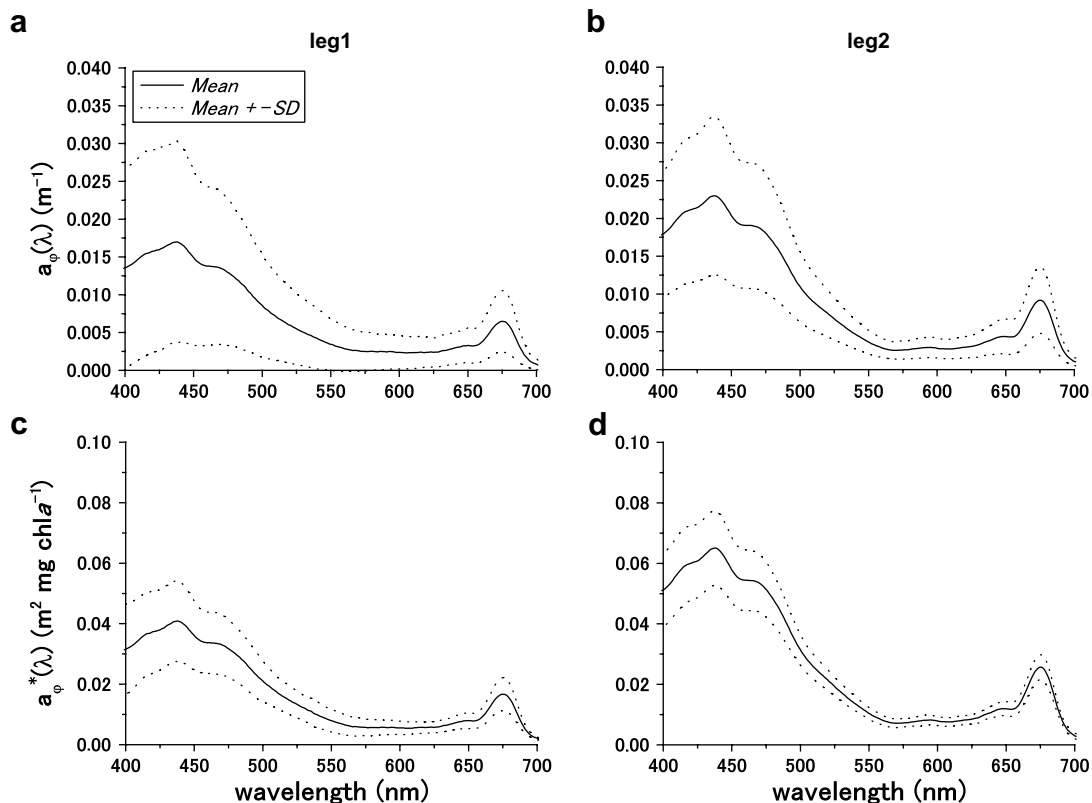
Fig. 7. (a, b) Phytoplankton absorption spectra $a_\varphi(\lambda)$. (c,d) chl a specific phytoplankton absorption spectra $a_\varphi^*(\lambda)$. Mean (solid curve) and the mean $\pm$ one standard deviation (SD) (dotted curve) are displayed.

species increasing their relative abundance through the decrease of other species abundances in the water column (Fig. 8b).

It is expected that smaller-size phytoplankton leads to less packaging effect (Morel and Bricaud, 1981; Bricaud and Morel, 1986; Bricaud et al., 1995). To evaluate the level of pigment packaging, we can use $a_\varphi^*(676)$ as an indicator of the packaging effect since the light absorption is not affected by accessory pigments at that wavelength. Values of $a_\varphi^*(676)$ for unpackaged pigments have the range of 0.023–0.029 m^2 mg chl a^{-1} (Johnsen et al., 1994; Moisan and Mitchell, 1999). Our results (Fig. 7) show that a small level of pigment

packaging was present for leg 1 ($a_\varphi^*(676) = 0.017$ m^2 mg chl a^{-1}) while no pigment packaging was measured for leg 2 ($a_\varphi^*(676) = 0.025$ m^2 mg chl a^{-1}). The values measured from autumn to early winter in our study area are thus higher than those measured in the region west of the Mackenzie river mouth in summer (0.014 m^2 mg chl a^{-1}; Wang et al., 2005), at Resolute Bay and in the Labrador Sea in the spring and fall (0.006 m^2 mg chl a^{-1} and 0.014 m^2 mg chl a^{-1}, respectively; Cota et al., 2003). This result suggests that pigment packaging is less important for our specific Arctic location and season and that the phytoplankton community
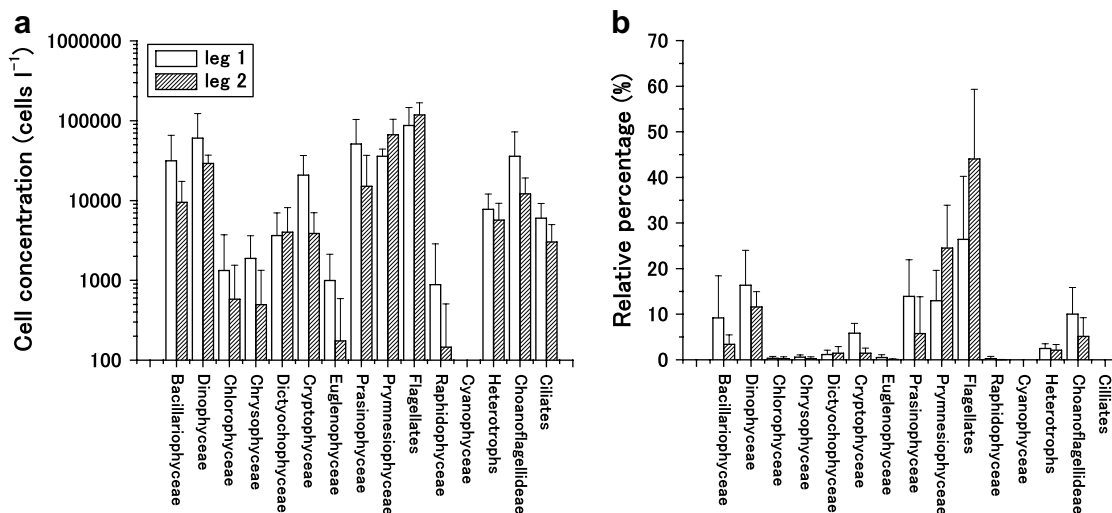

Fig. 8. Phytoplankton community composition. (a) Absolute cell concentration. (b) Relative percentage of each phytoplankton species to the total biomass. Error bars show one SD.

was generally more efficient to harvest light for leg 2. In addition, HPLC analysis indicated that the contribution of chl *b* to chl *a* was 19% and 44% for leg 1 and leg 2, respectively (see also discussion of Lovejoy et al., 2007) which is similar to ratios measured during the winter in the Atlantic where the dominant species are very small (Bricaud et al., 2004). This specific pigment is known to increase light absorption capacity (Moore et al., 1995; Bricaud et al., 2004) and its effect is observed in $a_\varphi(\lambda)$ and $a_\varphi^*(\lambda)$ spectra around 600 and 650 nm (Fig. 7).

The observed increase in $a_\varphi^*(\lambda)$ between the two legs can thus result from the modification of the phytoplankton community towards smaller cells having a larger $a_\varphi^*(\lambda)$, from a physiological adaptation of the smaller cells to better harvest light or from a combination of both. Our data set does not allow us to conclude on the specific process involved but it was already noted that phytoplankton can adapt its photosynthetic efficiency when submitted to a change of light intensity in the polar regions (Palmisano et al., 1986)

Smaller species that are more efficient to absorb light were thus present during leg 2. It is probable that the observed change in the phytoplankton community was the result of a species selection by the changing light level that was caused by a combination of decreasing sun elevation and the presence of a newly formed sea ice cover having an albedo varying between 2 and 80% depending on the type of ice present (Ehn et al., 2007).

The level of PP in the Arctic is a function of temperature, light intensity, and nutrient availability through the stability of the water column. Platt et al. (1982) indicated that temperature and light levels were more important to PP than nutrients using a data set acquired in northern Baffin Bay in September. This was confirmed by Harrison and Cota (1991) using an extended data set for the eastern Canadian Arctic. To examine this issue for our study area, chl *a*, $a_\varphi(443)$, and $a_\varphi^*(443)$ are plotted as a function of irradiance (Fig. 9). During leg 1, data points are particularly scattered for both chl *a* and $a_\varphi(443)$ (Fig. 9a,b). Since there was no clear dominant species of phytoplankton for leg 1 and as increased rate of phytoplankton biomass to irradiance is inferred to be different among phytoplankton species (Cota et al., 1994), the scattered data points shown in Fig. 9a,b are not surprising.

On the other hand, chl *a* and $a_\varphi(443)$ are positively correlated with irradiance for leg 2 ($r^2 = 0.41$ for both, $P < 0.0001$; Fig. 9a,b). These results demonstrate that the dominant small-size phytoplankton in this leg (i.e., Flagellates and Prymnesiophyceae) that contains a larger proportion of chl *b* relative to chl *a* tended to grow with increasing irradiance. However, variability in $a_\varphi^*(443)$ is not dependent on irradiance for both legs (Fig. 9c).

Fig. 10 shows $a_\varphi^*(443)$ as a function of temperature and nutrients. No correlation between $a_\varphi^*(443)$ and temperature is found for both legs. This could result from the fact that different dominant species were present in our study area compared to Baffin Bay (i.e., Bacillariophycae; Platt et al., 1982). On the other hand, our results based on stepwise regression analysis demonstrate that $a_\varphi^*(443)$ is significantly correlated with $NO_3 + NO_2$ and this correlation is higher ($r^2 = 0.12$, $P < 0.001$) than with phosphate and silicates for both legs (see Table 3 for details). This is contrary to lower latitude results that suggested a negative correlation (see discussion of Bricaud et al., 1995). So for our specific environmental conditions of very low irradiance and cold temperature during the early winter period, $a_\varphi^*(443)$ might be more sensitive to changes in nutrients than by the light intensity and temperature since the variability in these two parameters is small in addition to their small absolute values. More work on phytoplankton physiology for Arctic waters is thus necessary to understand the contribution of primary production to the Arctic carbon cycle.
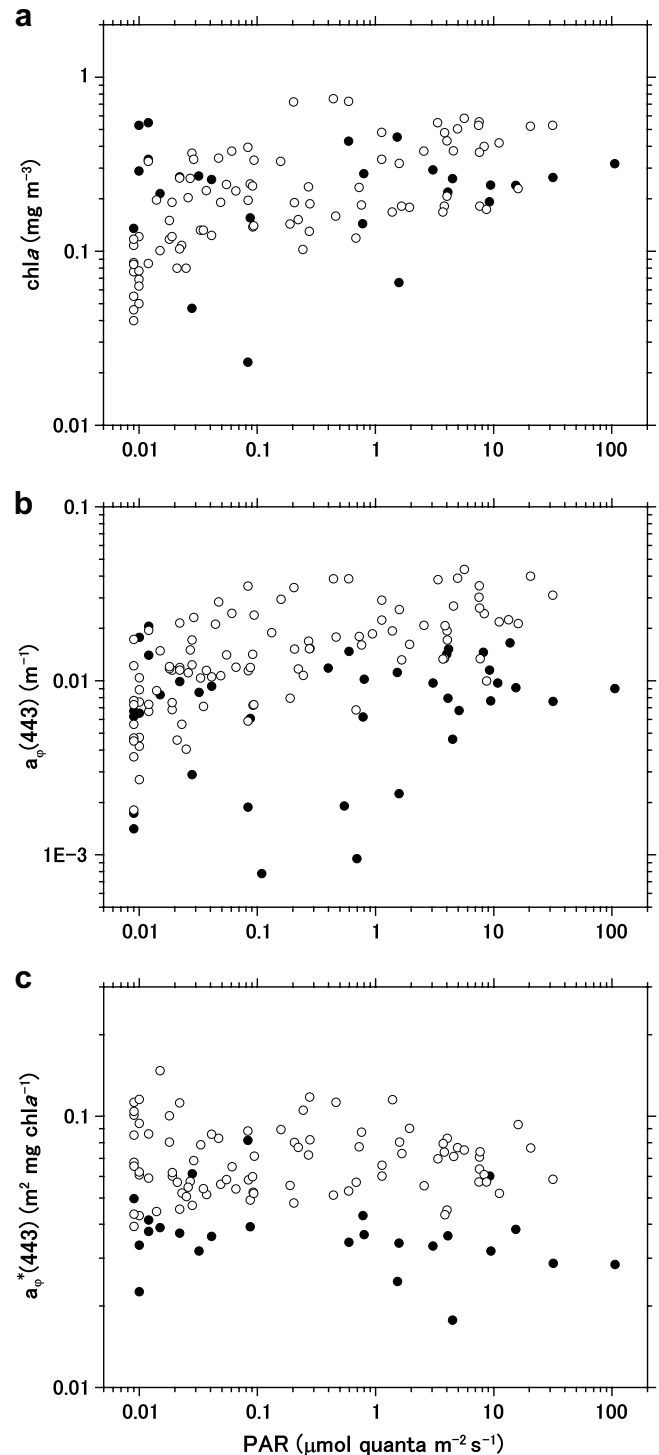

Fig. 9. Scatter-plot of (a) chl *a*, (b) $a_\varphi(443)$, and (c) $a_\varphi^*(443)$ as a function of irradiance. See Fig. 2 for symbols.

4. Conclusions

The Mackenzie River, the fourth largest river discharging into the Arctic, has an important role for freshwater input with nutrient supply to the coastal Beaufort Sea. Our results showed that the river plume influences the optical properties in the surface layer alone (approximately <10 m) and that this influence is still left in the autumn and early winter seasons over the entire southern Beaufort
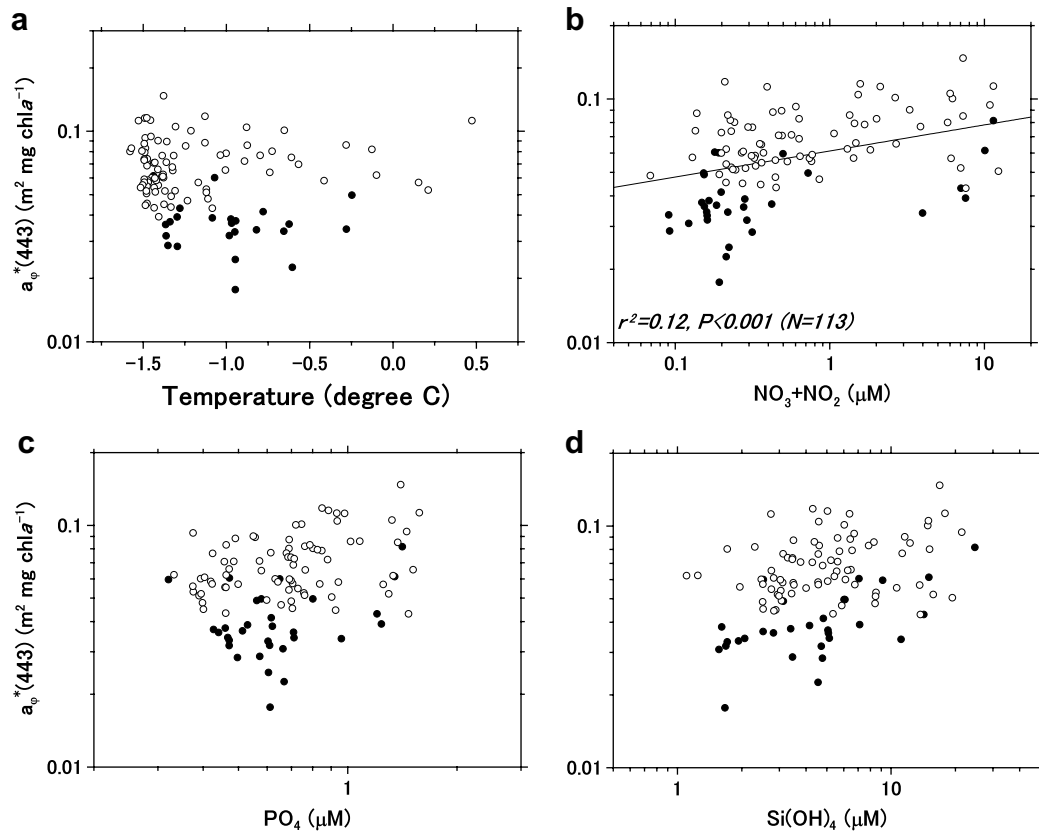
Fig. 10. Scatter-plot of $a_\varphi^*(443)$ as a function of (a) temperature, (b) $NO_3 + NO_2$, (c) PO_4, and (d) $Si(OH)_4$. The best fit for all data points is displayed on Fig. 10b. See Fig. 2 for symbols. The statistical results based on stepwise regression analysis are shown in Table 3.

Table 3
Stepwise regression analysis of chl a specific absorption coefficient of phytoplankton with environmental factors (light, temperature, and nutrients). $^*P < 0.01$, $^{**}P < 0.005$, $^{***}P < 0.001$.

Selected parameters	1	2	3***	4*	5***	3 + 4 + 5**	1 + 3 + 4 + 5**	2 + 3 + 4 + 5**	1 + 2 + 3 + 4 + 5*
Intercept	−1.235	−1.267	−1.209	−1.197	−1.355	−1.287	−1.286	−1.303	−1.302
^{1}Log$_{10}$(I)	−0.017						0.003		0.002
^{2}T		−0.037						−0.019	−0.018
^{3}Log$_{10}$(NO$_3$ + NO$_2$)			0.098			0.035	0.035	0.033	0.033
^{4}Log$_{10}$(PO$_4$)				0.211		0.109	0.114	0.120	0.123
^{5}Log$_{10}$(Si(OH)$_4$)					0.190	0.120	0.122	0.114	0.116
Adjusted r^2	0.00	0.00	0.12	0.06	0.10	0.12	0.11	0.15	0.15
F	1.25	0.89	14.71	7.42	11.61	5.65	4.20	4.26	3.38
P-value	0.2664	0.3466	0.0002	0.0076	0.0009	0.0013	0.0035	0.0032	0.0075

sea region. While strong light absorption by terrigeneous CDOM (up to 84% of $a_{t-w}(443)$ for both legs) is relatively constant, the light absorption by phytoplankton tended to increase from autumn when open water still existed to early winter when sea ice cover was formed. This is probably caused by biological selection of smaller-sized cells that are either already more efficient or capable to adapt their physiology to harvest the available light. The phytoplankton light absorption capacity showed a significant positive correlation with $NO_3 + NO_2$ which is in contrast to previous results from lower latitudes data sets. This probably results from a combination of very limited available light and low water temperatures making $a_\varphi^*(\lambda)$ more sensitive to nutrient supply.

The important implication of this study is that the phytoplankton community structure will adapt to the new physical environment that will result from a reduced ice cover, a shorten ice season and concurrent increases in freshwater input from land (McClelland et al., 2006) that includes larger amounts of nutrients (Holms et al., 2008) due to melting permafrost (Camill, 2005). This could lead to possible higher trophic levels effects through a change in the food web structure.

542

546 *A. Matsuoka et al. / Estuarine, Coastal and Shelf Science 82 (2009) 537–546*

through the program of Arctic research projects using IARC (International Arctic Research Center)–JAXA Information System (IJIS), and by the National Institute of Polar Research (NIPR) of Japan.

References

Aagaard, K., Carmack, E.C., 1989. The role of sea ice and other fresh water in the arctic circulation. Journal of Geophysical Research 94, 14485–14498.
Arrigo, K.R., Worthen, D., Schnell, A., Lizotte, M.P., 1998. Primary production in southern ocean waters. Journal of Geophysical Research 103, 15587–15600.
Babin, M., Stramski, D., Ferrari, G.M., Claustre, H., Bricaud, A., Obolensky, G., Hoepffner, N., 2003. Variations in the light absorption coefficients of phytoplankton, nonalgal particles, and dissolved organic matter in coastal waters around Europe. Journal of Geophysical Research 108, doi:10.1029/2001JC000882.
Bélanger, S., Xie, H., Krotkov, N., Larouche, P., Vincent, W.F., Babin, M., 2006. Photomineralization of terrigenous dissolved organic matter in Arctic coastal waters from 1979 to 2003: interannual variability and implications of climate change. Global Biogeochemical Cycles 20, doi:10.1029/2006GB002708.
Bérard-Therriault, L., Poulin, M., Bossé, L., 1999. Guide d'identification du phytoplancton marin de l'estuaire et du golfe du Saint-Laurent incluant également certains protozoaires. Canadian Special Publication of Fisheries and Aquatic Sciences 128, 1–387.
Bricaud, A., Morel, A., 1986. Light attenuation and scattering by phytoplankton cells: a theoretical modeling. Applied Optics 25, 571–580.
Bricaud, A., Babin, M., Morel, A., Claustre, H., 1995. Variability in the chlorophyll-specific absorption coefficients of natural phytoplankton: analysis and parameterization. Journal of Geophysical Research 100, 13321–13332.
Bricaud, A., Claustre, H., Ras, J., Oubelkheir, K., 2004. Natural variability of phytoplanktonic absorption in oceanic waters: influence of the size structure of algal populations. Journal of Geophysical Research 109, doi:10.1029/2004JC002419.
Bricaud, A., Morel, A., Babin, M., Allai, K., Claustre, H., 1998. Variations of light absorption by suspended particles with chlorophyll a concentration in oceanic (Case 1) waters: analysis and implications for bio-optical models. Journal of Geophysical Research 103, 31033–31044.
Camill, P., 2005. Permafrost thaw accelerates in boreal peatlands during late-20th century climate warming. Climate Change 68, 135–152.
Carmack, E.C., Macdonald, R.W., 2002. Oceanography of the Canadian Shelf of the Beaufort Sea: a setting for marine life. Arctic 55, 29–45.
Carmack, E.C., Macdonald, R.W., Jasper, S., 2004. Phytoplankton productivity on the Canadian Shelf of the Beaufort Sea. Marine Ecology Progress Series 277, 37–50.
Claustre, H., Bricaud, A., Babin, M., Bruyant, F., Guillou, L., Gall, F.L., Marie, D., Partensky, F., 2002. Diel variations in Prochlorococcus optical properties. Limnology and Oceanography 47, 1637–1647.
Cleveland, J.S., Weidemann, A.D., 1993. Quantifying absorption by aquatic particles: a multiple scattering correction for glass-fiber filters. Limnology and Oceanography 38, 1321–1327.
Cota, G.F., Harrison, W.G., Platt, T., Sathyendranath, S., Stuart, V., 2003. Bio-optical properties of the Labrador Sea. Journal of Geophysical Research 108, doi:10.1029/2000JC000597.
Cota, G.F., Smith Jr., W.O., Mitchell, B.G., 1994. Photosynthesis of Phaeocystis in the Greenland Sea. Limnology and Oceanography 39, 948–953.
Ehn, J.K., Hwang, B.J., Galley, R., Barber, D.G., 2007. Investigations of newly formed sea ice in the Cape Bathurst polynya: 1. Structural, physical, and optical properties. Journal of Geophysical Research 112, doi:10.1029/2006JC003702.
Falkowski, P.G., Raven, J.A., 1997. Aquatic Photosynthesis. Oxford University Press, Blackwell, 375 pp.
Fujiki, T., Taguchi, S., 2002. Variability in chlorophyll a specific absorption coefficient in marine phytoplankton as a function of cell size and irradiance. Journal of Plankton Research 24, 859–874.
Gordon, H.R., McCluney, W.R., 1975. Estimation of the depth of sunlight penetration in the sea for remote sensing. Applied Optics 14, 413–416.
Grasshoff, K., 1999. Methods of Seawater Analysis, third ed. Wiley-VCH, Weinheim, New York. 159–228.
Harrison, W.G., Cota, G.F., 1991. Primary production in polar waters: relation to nutrient availability. Polar Research 10, 87–104.
Holm-Hansen, O., Lorenzen, C.J., Holms, R.W., Strickland, J.D.H., 1965. Fluorometric determination of chlorophyll. Journal de Conseil International pour l'Exploration de la Mer 30, 3–15.
Holms, R.M., McClelland, J.W., Raymond, P.A., Frazer, B.B., Peterson, B.J., Stieglitz, M., 2008. Lability of DOC transported by Alaskan rivers to the Arctic Ocean. Geophysical Research Letters 35, doi:10.1029/2007GL032837.
Huot, Y., Babin, M., Bruyant, F., Grob, C., Twardowski, M.S., Claustre, H., 2007. Relationship between photosynthetic parameters and different proxies of phytoplankton biomass in the subtropical ocean. Biogeoscience 4, 853–868.
Johnsen, G., Nelson, N.B., Jovine, R.V., Prezelin, B.B., 1994. Chromoprotein- and pigment-dependent modeling of spectral light absorption in two dinoflagellates, Prorocentrum minimum and Heterocapsa pygmaea. Marine Ecology Progress Series 114, 245–258.

Kirk, J.T.O., 1994. Light and Photosynthesis in Aquatic Ecosystems. Cambridge University Press, New York, 509 pp.
Kishino, M., 1994. Interrelationships between light and phytoplankton in the sea. In: Spinrad, R.W., Carder, K., Perry, M.J. (Eds.), Ocean Optics. Oxford University Press, New York, pp. 73–92.
Kishino, M., Takahashi, M., Okami, N., Ishimaru, S., 1985. Estimation of the spectral absorption coefficients of phytoplankton in the sea. Bulletin of Marine Science 37, 634–642.
Longhurst, A., Sathyendranath, S., Platt, T., Caverhill, C., 1995. An estimate of global primary production in the ocean from satellite radiometer data. Journal of Plankton Research 17, 1245–1271.
Lovejoy, C., Vincent, W., Bonilla, S., Roy, S., Martineau, M.-J., Terrado, R., Potvin, M., Messana, R., Pedos-Alio, C., 2007. Distribution, phylogeny, and growth of cold-adapted picoprasinophytes in Arctic seas. Journal of Phycology 43, 78–89.
Lund, J.W.G., Kipling, C., LeCren, E.D., 1958. The inverted microscope method of estimating algal numbers and the statistical basis of estimations by counting. Hydrobiologia 11, 143–170.
McClelland, J.W., Déry, S.J., Peterson, B.J., Holms, R.M., Wood, E.F., 2006. A pan-arctic evaluation of changes in river discharge during the latter half of the 20th century. Geophysical Research Letters 33, doi:10.1029/2006GL025753.
Macdonald, R., Yu, Y., 2006. The Mackenzie Estuary of the Arctic Ocean. In: Wangersky, P.J. (Ed.), The Handbook of Environmental Chemistry. Springer, Berlin, pp. 91–120.
Macdonald, R.W., Wong, C.S., Erickson, P.E., 1987. The distribution of nutrients in the Southeastern Beaufort Sea: implications for water circulation and primary production. Journal of Geophysical Research 92, 2939–2952.
Matsuoka, A., Huot, Y., Shimada, K., Saitoh, S., Babin, M., 2007. Bio-optical characteristics of the Western Arctic Ocean: implications for ocean color algorithms. Canadian Journal of Remote Sensing 33, 503–518.
Matsuoka, A., Larouche, P., Hirawake, T., Garneau, M.-E., Simpson, K., Saitoh, S., Hattori, H., 2006. Dramatic change of bio-optical properties before and after sea ice production in the mouth of the Mackenzie River and the Cape Bathurst polynya regions, Canadian Arctic.Proc. SPIE Int. Soc. Opt. Eng.. Ocean Optics 18 [CD ROM], Washington, D.C., 60064.
Mitchell, B.G., Holm-Hansen, O., 1987. RACER: optical prediction of photobiological properties. Antarctic Journal of the United States 22, 145–147.
Moisan, T.A., Mitchell, B.G., 1999. Photophysiological acclimation of Phaeocystis Antarctica Karsten under light limitation. Limnology and Oceanography 44, 247–258.
Moore, L.R., Goericke, R., Chisholm, S.W., 1995. Comparative physiology of Synechococcus and Prochlorococcus: influence of light and temperature on growth, pigments, fluorescence, and absorptive properties. Marine Ecology Progress Series 116, 259–275.
Morel, A., 1991. Light and marine photosynthesis: a spectral model with geochemical and climatological implications. Progress in Oceanography 26, 263–306.
Morel, A., Bricaud, A., 1981. Theoretical results concerning light absorption in a discrete medium, and application to specific absorption of phytoplankton. Deep-Sea Research 28A, 1375–1393.
Nieke, B., Reuter, R., Heuermann, R., Wang, H., Babin, M., Therriault, J.C., 1997. Light absorption and fluorescence properties of chromophoric dissolved organic matter (CDOM), in the St. Lawrence Estuary (Case 2 waters). Continental Shelf Research 17, 235–252.
Ohi, N., Mizobuchi, A., Taguchi, S., 2006. Light absorption of Isochrysis galbana (Prymnesiophyceae) under a day–night cycle with ultraviolet radiation. Marine Ecology Progress Series 316, 85–93.
Palmisano, A.C., SooHoo, J.B., SooHoo, S.L., Kottmeier, S.T., Craft, L.L., Suillivan, C.W., 1986. Photoadaptation in Phaeocystis pouchetii advected beneath annual sea ice in McMurdo Sound, Antarctica. Journal of Plankton Research 8, 891–906.
Parsons, T.R., Maita, Y., Lalli, C.M., 1984. A Manual of Chemical and Biological Methods for Seawater Analysis. Pergamon Press, Toronto, 173 pp.
Platt, T., Sathyendranath, S., 1988. Oceanic primary production: estimation by remote sensing at local and regional scales. Science 241, 1613–1620.
Platt, T., Harrison, W.G., Irwin, B., Horne, E.P., Gallegos, C.L., 1982. Photosynthesis and photoadaptation of marine phytoplankton in the Arctic. Deep-Sea Research 29, 1159–1170.
Sathyendranath, S., Platt, T., Horne, E.P.W., Harrison, W.G., Ulloa, O., Outerbridge, R., Hoepffner, N., 1991. Estimation of new production in the ocean by compound remote sensing. Nature 353, 129–133.
Stein, R., Macdonald, R.W., 2004. The Organic Carbon Cycle in the Arctic Ocean. Springer, Berlin, 363 pp.
Stramski, D., Reynolds, R.A., 1993. Diel variations in the optical properties of a marine diatom. Limnology and Oceanography 38, 1347–1364.
Tomas, C.R., 1997. Identifying Marine Phytoplankton. Academic Press, San Diego, 858 pp.
Utermöhl, H., 1931. Neue Wege in der quantitativen Erfassung des Palnktons (Mit besondere Bericksichtigung des Ultraplankton). Zwecke und Ziele der Internationalen Vereinigung für theoretische und angewandte Limnologie 5, 567–595.
Wang, J., Cota, G.F., Ruble, D.A., 2005. Absorption and backscattering in the Beaufort and Chukchi Seas. Journal of Geophysical Research 110, doi:10.1029/2002JC001653.